Original Research Article

CrystallographicBenchmarking on Diffraction Pattern Profiling of Polymorphs-$TiO_2$by WPPF for Pigment and Acrylic Paint

ABSTRACT

At a very low temperature high crystalline phase ofTiO_2 best-fitted strain anatase was synthesized by peptization which was the prime object of this study. Unresolved parameters were investigated by theX-ray diffraction (XRD) technique employed for lattice parameters, crystallite size, lattice volume, strain, crystal structure, d-spacing and percentage of phase inweight fraction. 54.40 % anatase, 29.10 % brookite and 16.50 % rutilecrystalline phase were found by whole powder pattern fitting (WPPF-Rietveld's refinement)methodand lattice volume of anatase 137.150, brookite 267.079 and rutile 62.901 $Å^3$ as well the crystal strain 0.307, 0.45 and 0.28 % of anatase, brookite and rutile polymorph-TiO_2found respectively. The calculated lattice parameters of the anatase are $\alpha=\beta=\gamma=90.0°$; a=b=3.8056Å, c=9.470Å and predominant (101), (004) and (200) miller indices with diffracted angle(2Ɵ)25.38, 37.26 and 48.22 observed.The average crystallite size was 7.39 nm which confirmed the formation of nano-crystal-TiO_2due tothe highly dispersed on medium.The percentage ofstrain of the individual polymorphs of TiO_2showsthebest fit used for the pigment and acrylic paint.

Keywords: Acrylic Paint, Anatase, Brookite, Pigment, Rutile

1. Introduction

Pablo Picasso turned forty in 1921, and not long after an industrial process for making titanium white pigment was created and made public [1]. He has been employing titanium white as a photocatalyst in his work [2] which might seriously harm his reputation and he wasn't the only one [1]. Apart from its application in paintings [3-6], titanium white has also been included in plastic art pieces and photographic paper (resin-coated prints), resulting in issues with deterioration [7, 8]. An established photocatalyst is titanium dioxide. A series of reactions may result in the creation of radicals when titanium dioxide absorbs UV light. These free radicals can damage nearby pigment which can lead to an organic medium breakdown and embrittlement, gloss lossor chalking. The colour may also change when dye-stuffs, pigments or colourants are used [9–11]. Pigments made of titanium dioxide have been appropriately used to give a variety of materials opacity or whiteness. Various sectors, including plastics, paints, paper and inks can utilize them [12]. Because of its high refractive index and capacity to absorb UV radiation, TiO_2 has several remarkable properties that have earned it an exceptional reputation among other white pigments. These advantages include effective light scattering and product durability. Additionally, because it is non-toxic there is less risk to safety and health, making it suitable for use in a variety of applications [13].TiO_2 nanoparticles exhibit distinct optical behaviours in comparison to traditional TiO_2 pigments. TiO_2nanoparticle optical characteristics are explained by the Rayleigh theory of light scattering. Small particles more effectively scatter light at shorter wavelengths, according to this theory. Additionally, the anatase form of TiO_2nanoparticlephotocatalytic activity has been used to create a variety of materials with theself-cleaning feature [14]. The industry has paid a lot of attention lately to self-cleaning coatings that use photocatalytic titanium dioxide nanoparticles. TiO_2 nanoparticles have a strong oxidation capacity that can be utilized to eradicate dirt stains or kill bacteria that have adhered to the walls. Moreover, when such a coating is put on external surfaces, the super-hydrophilic

nature of dirt and stains can make it simple for water or rainfall to wash them away [15, 16]. Because of their incredibly high surface area to particle size ratio, nanoparticles also have a strong potential to agglomerate as well as magnetic and nanorod properties [41, 42, 43]. Thus, dispersing the nanoparticles without agglomerating in the organic binders is essential for creating an appropriate TiO_2-modified paint. The surfaces of the TiO_2 nanoparticles are coated with sufficient precipitated inorganic compounds, such as $SiO_2$and Al_2O_3, to enhance their dispersion and decrease their photoactivity [16]. The crystalline phase percentage of nanomaterials is also effective to their inherent property [29-32]Commercially obtainable three TiO_2 nanoparticles have been used as additions in varying quantities to white acrylic water-based paint to study how this improves the paint's ability to clean itself.For the preparation of the polymorphs TiO_2, a different route is also applied such as peptization [17], hydrothermal or solvothermal [33, 38], sol-gel [34], etc are followed.The primary focus of this studyis the ultrafine highly crystalline polymorph-TiO_2 synthesized in the forms of rutile, brookite and anatasebya unique simple route.

2. Materials and Method

Titanium isopropoxide (TTIP), Ethanol, Nitric acid and Isopropyl alcohol (IP)are purchased from Sigma-Aldrich and De-ionized water is collected from IPCRD, IGCRT, BCSIR. The precursor solution TTIP and IP was mixed with a 1: 3 ratio (v/v) and stirred for 10.00 minutes. On another 500.00 ml beaker add 250.00 ml DI water and maintain pH for 2.0 to 2.5. The prepared two solutions were mixed with and followed the 400.00 rpm and 65 ◦C for 17-18h peptization of the gel was formed. After the peptization, the gel volume decreases to 50.0 cm^3. The final suspension was washed with ethanol with centrifuged at 8000.00 rpm several times. The precipitated dried at oven 60.0 $^{\circ}$C a white fine powder was obtained. After preparing the sample at 9.0 hours the crystallographic measurement techniques were employedat room temperature.

3. Characterization

The Smart-Lab SE, a versatile X-ray Diffractometer manufactured by Rigaku in Japan was used to observe X-ray diffraction patterns. The instrument was equipped with a 40 KV x 50 mA (2.00 kW) source, 10.00mm CBO-BB optics, and a K_β filter made of Ni (28). In this case, the procedure was executed with a step size of 0.001^0 (speed of 05^0/min), a HyPix-400 (HPAD-1D) detector operating in standard modeand collecting 10^6/pixel rate data. The crystallographic structure and lattice parameters of a material are ascertained by subjecting the material to irradiation with incoming X-rays and subsequently measuring the diffraction angles and intensities of the X-rays that exit the material[39]. The analysis was conducted on the powdered material at a temperature of 25.00 ℃, which corresponds to room temperature. X-ray diffraction is commonly used to determine the crystal structure of polymorph-TiO_2. The Debye-Scherrer formula has been utilized to determine the size of crystallites by X-ray diffraction examination.

$$D = \frac{0.9\lambda}{\beta cos\theta}$$

Where, D = Crystal size, λ = Wavelength of the X-ray (λ=0.1541 nm), β = Full width at half maximum and θ = Diffraction angle [17].

Bragg`s law has been applied for the determination of the d-spacing values (inter-planar distance between atoms)

$$d = \frac{\lambda}{2sin\theta}$$

Table 1 is utilized for the listing of the crystal size and d-spacing values that are determined. The quantitative analysis of thesynthesized powder-TiO_2 was determined using the WPPF technique (Whole powder pattern fitting method) given in Table 6.

4. Result and Discussion

The X-ray crystallographic diffractogram revealed three prominent diffractions at 2Θ= 25.38, 37.26 and 48.22 with corresponding intensities of 3927, 554and 927 counts per second (cps). On the other hand, two minor diffractions were also observed at 2Θ= 30.65 and 54.5 with intensities of 227 and 801 cps. The main three diffractions 25.38, 37.26 and 48.22 were responsible for anatase-TiO_2[ICDD Card No # 01-083-5914]and another two diffractions 30.65 and 54.5 were responsible for brookite and rutile-TiO_2 polymorphs respectively which as shown in Fig 1.

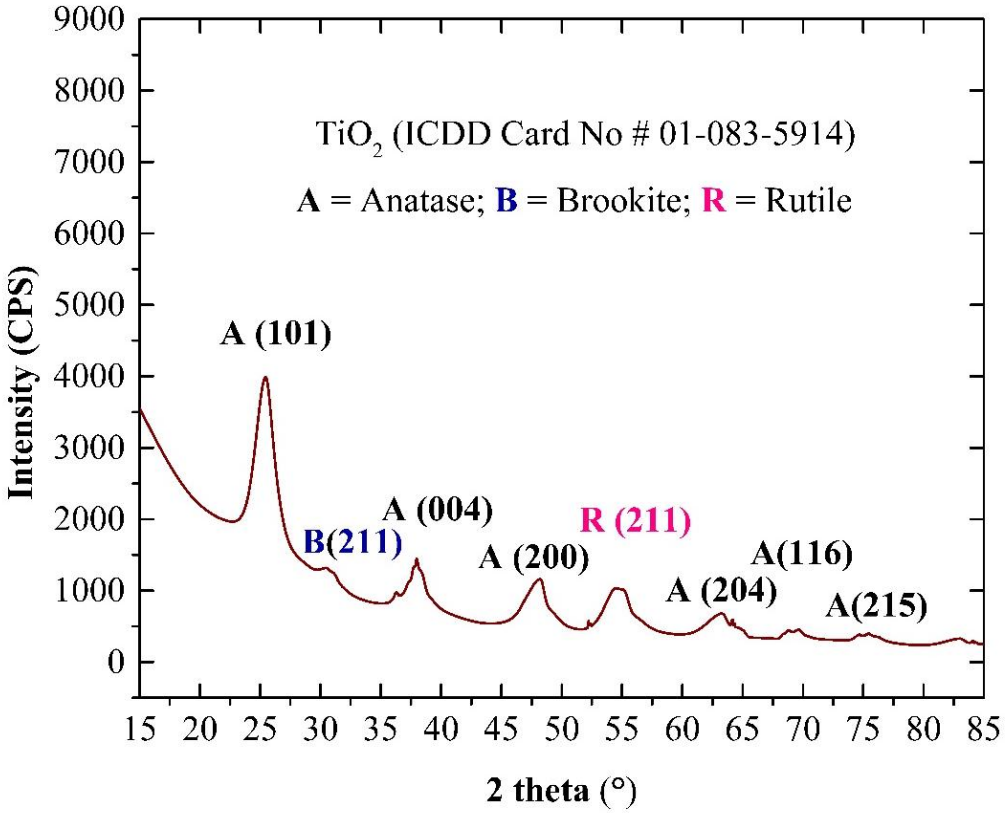

Fig. 1. X-ray diffractogram of synthesizedTiO_2at room temperature

The minor diffraction was found at 2Θ= 63.41, 69.43 and 75.73 with intensity of 457, 76 and 58 cps which is also responsible for the prominent anatase [ICDD Card No # 01-083-5914].

Table 1. The calculation of the grain size of TiO_2

Diffraction angle (2Θ)	Theta (Θ)	(hkl)	FWHM (radians)	Size of the crystallite (D± 0.01) nm	d-spacing (d± 0.001) (nm)
25.38	12.69	(1 0 1)	1.453	5.87	0.35056

37.26	18.63	(0 0 4)	0.79	11.20	0.24110
48.22	24.11	(2 0 0)	1.792	5.08	0.18858

Table 1, shows that the three main diffractions were observed at 25.38, 37.26 and 48.22 with the prominent respective Miller indices (101), (004) and (200). The crystallite size was determined by the Debye-Scherrer formula with three respective diffractions such as 5.87, 11.20 and 5.08 nm. The calculated average crystallite size was 7.39nm which confirmed the formation of nanocrystal-TiO_2 that shows an outstanding dispersion on paint medium[12]. The interplanar distance (d-spacing) was also calculated by the Bragg formula of the main three intense diffractions. The calculated d-spacing at 25.38, 37.26 and 48.22 were 0.35056, 0.24110 and 0.18858 nm. This d-spacing exhibits the uniformity of the nanocrystal-TiO_2[17, 31, 36].

Table 2. Peak profiling of TiO_2 by diffraction angle

Diffraction angle (2Θ)	Theta (Θ)	1000× $Sin^2Θ$	Reflection	Remarks
25.38	12.69	48.25	(1 0 1)	$1^2 + 0^2 + 1^2 = 2$
37.26	18.63	102.05	(0 0 4)	$0^2 + 0^2 + 4^2 = 16$
48.22	24.11	166.863	(2 0 0)	$2^2 + 0^2 + 0^2 = 4$

Table 2, exhibits the peak profiling of the TiO_2 by diffraction position(Θ). Three significant values of the peak profiling were 48.25, 102.50 and 166.83 observed at the 2Θ= 25.38, 37.26 and 48.22. The peak profiling and remarks value interval also ensured the particles were uniformly distributed onto the plane into the crystal system [17, 32, 37].

Table 3. Peak profiling of TiO_2 by inter-planner (d-spacing) distance

Diffraction angle (2Θ)	Inter-planner distance (d), (Å)	$1000/d^2$	Reflection	Remarks

25.38	3.5056	81.37	(1 0 1)	$1^2 + 0^2 + 1^2 = 2$
37.26	2.4110	172.05	(0 0 4)	$0^2 + 0^2 + 4^2 = 16$
48.22	1.8858	281.21	(2 0 0)	$2^2 + 0^2 + 0^2 = 4$

Table 3, exhibits the peak profiling of the TiO_2 by d-spacing. The peak profiling was 81.37, 172.05 and 281.21 observed at the 2Θ= 25.38, 37.26 and 48.22 values with respective d-spacing 3.5056, 2.4110 and 1.8858 Å. Three significant interval values from peak profiling ensure that the crystals are well-growth onto plane[17] for their uniform distribution as well as remarks value.

Table 4. An analysis of the experimental (Exp.) and standard (Std.) diffraction data is being conducted for comparison.

Diffraction angle (2Θ)		Inter-planer distance (d) (Å)		Lattice parameters of Std.
(Exp.)	(Std.)	(Exp.)	(Std.)	Space Group: I41/amd (141) a=b= 3.7845 Å c= 9.5111 Å; α=β=γ=90.0°; c/a: 2.513, Volume= 136.22 Å^3. [ICDD Card No # 01-083-5914]
25.38	25.307	3.5056	3.516360	
37.26	37.804	2.4110	2.377780	
48.22	48.042	1.8858	1.892250	

Table 4, displays the comparison between experimental data and standard data from ICDD (Card No # 01-083-5914). The standard diffractions were detected at 25.307, 37.804 and 48.042 whereas the synthesis TiO_2 diffraction was seen at 2Θ= 25.38, 37.26 and 48.22 which closely matches the standard data.The ICDD bilographic shown as Space Group: I41/amd (141)a=b= 3.7845 Å c= 9.5111 Å; α=β=γ=90.0°; c/a: 2.513, Volume= 136.22 Å.Alternatively, the d-spacing values of the standard data were observed at 3.516360, 2.377780 and 1.892250 Å which is also similar to the synthesized TiO_2 d-spacing 3.5056, 2.4110 and 1.8858 Å.

Table 5. Calculation of Percentage of Crystallinity

2Θ (Exp.)	Norm. I. (%) (Exp.)	Percent of Crystallinity (%)	2Θ (Std.)	Norm. I. (%) (Std.)	Percent of Crystallinity (%)
25.38	100.00		25.307	100.00	
37.26	14.00	53.80	37.804	18.00	70.20
48.22	72.00		48.042	24.50	

Table 5, represents the normalized intensity (I.) of the synthesized TiO_2 and ICDD standard. The I. calculated values of synthesized TiO_2 were 100.00, 14.0 and 72.00 at the diffraction position 2Θ= 25.38, 37.26 and 48.22. So, the crystallinity was observed at 53.80% whereas the ICDD standard shows the crystallinity at 70.20% confirming that it is the highly ordered [17] in a three-dimensional lattice.

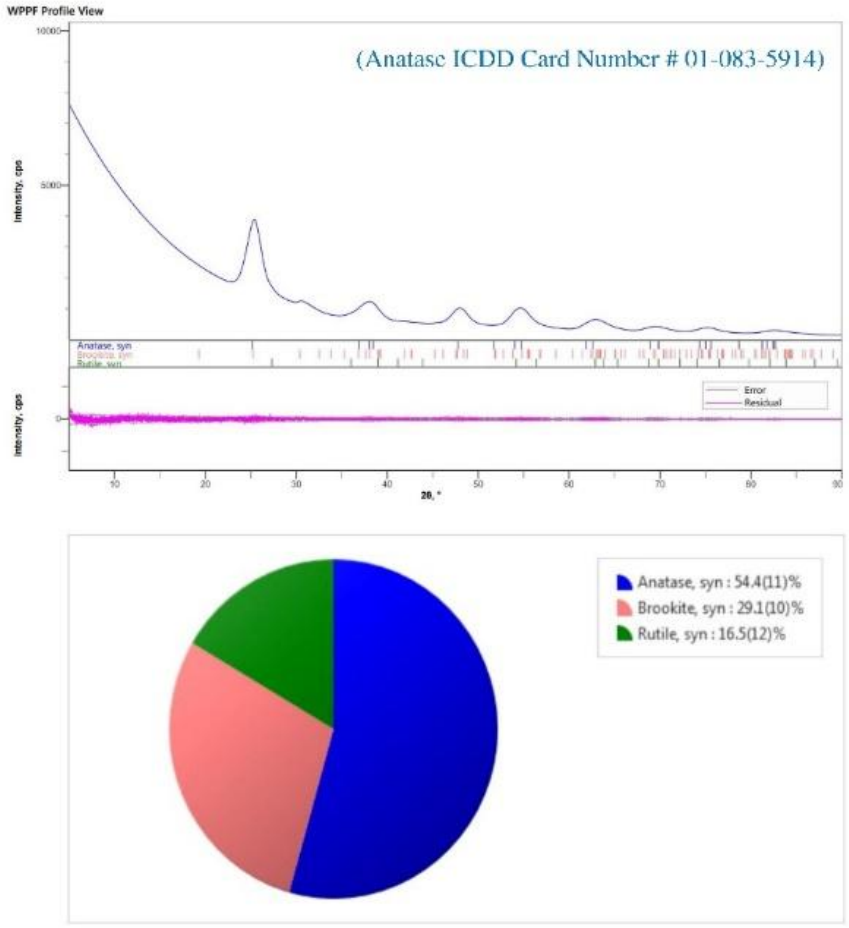

Fig. 2. Quantitative analysis of Polymorph-TiO_2 by the WPPF (Whole powder pattern fitting) method

Fig. 2, Shows the phase percentage (%) of the crystalline polymorphs of TiO_2 that is determined by the WPPF method. The calculated phase percentage observed that 54.40 % anatase, 29.10 % brookite and 16.50 % rutile were found at the pattern fitting condition Rwp, 9.84 %, Rp 7.01 %, S 0.4092, χ^2 0.1674.

Table 6. Rietveld's refinement of the polymorph-TiO_2 by WPPF

Rwp (%)	Rp (%) and S	Weight fraction, Wt (± 0.01) %	Lattice volume (± 0.01) Å³	Strain (± 0.001) %	Lattice parameters
			Anatase		
9.84	7.01 0.4092	54.40	137.150	0.307	α=β=γ=90.0° a=b=3.8056Å, c=9.470Å
			Brookite		
9.84	7.01 0.4092	29.1	267.079	0.45	α=β=γ=90.0° a=9.186 Å, b=5.500Å, c=5.287Å
			Rutile		
9.84	7.01 0.4092	16.50	62.901	0.28	α=β=γ=90.0° a=b=4.613 Å, c=2.956 Å

Table 6, shows the Rietveld refinement of the polymorph-TiO_2 at the same pattern-fitting condition whereas the calculated lattice volume of anatase 137.150, brookite 267.079 and rutile 62.901 Å³ as well as the crystal strain 0.307, 0.45 and 0.28 % of anatase, brookite and rutile polymorph respectively. The strain ensured that the stability of crystalline polymorph-TiO_2 was suitable for the paint medium. The crystal lattice parameters are also calculated by Rietveld refinement, whereas anatase α=β=γ=90.0°, a=b=3.8056Å, c=9.470 Å; brookite α=β=γ=90.0°, a=9.186 Å b=5.500Å, c=5.287Å; rutile α=β=γ=90.0°, a=b=4.613 Å, c=2.956 Å; for its fitted data confirmed the uniformity of the crystal are best suitable to the UV and other radiation that was various prominent application for the pigment and acrylic paint.

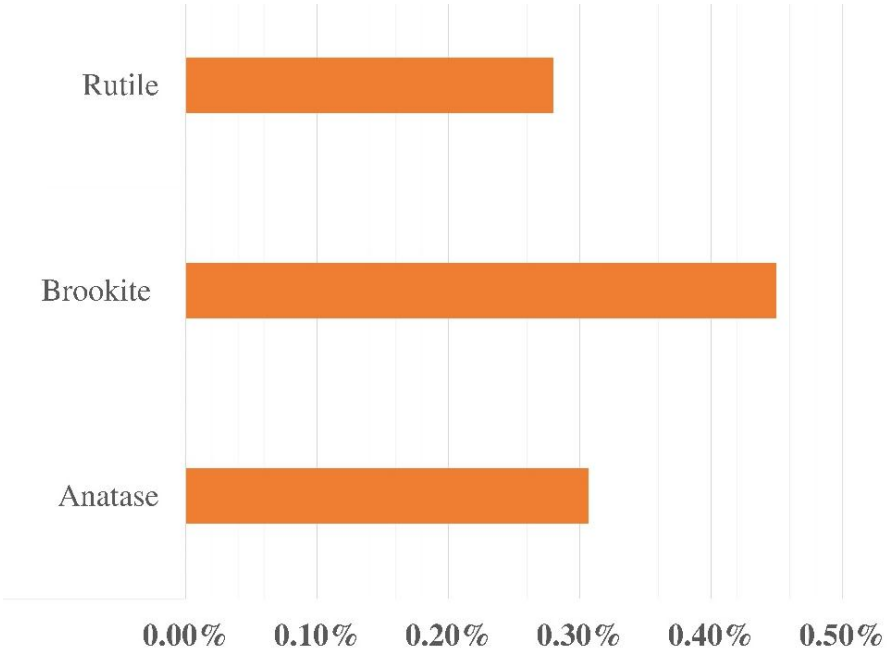

Fig. 3. Strain curve of polymorph-TiO_2

Fig. 3, strain curve shows that the high strain easily decomposed the preferred orientation (001) and turned into an amorphous[35];the anatase strain (0.307 %) curve is more stable than brookite (0.45 %)cure as well as rutile. So, the anatase strain is preferred to the paint for its antimicrobial and light scattering properties as well as self-cleaning for the rutile polymorph strain[40].The application of TiO_2 coating is possible on various surfaces including the surface of indoor and outdoor buildings, metallic objects, wooden frames and domestic and professional instruments[18]. Rutile and anatase are the two polymorphs of TiO_2 but the rutile form of TiO_2 cannot boost implemented photocatalytic activity [18,19]. On the contrary, the anatase prominent phase form can enhance the photocatalytic activity when mixed with paintas well as film formation, increasing coverage area, hiding, smooth surface area and structural modificationdue to its contrast ratio, opacity, refractive index and viscosity [20,21, 38, 40, 43]. The addition of TiO_2 into the paint can modify the paint performance traits including peeling, wake retention, cracking, flaking and muckraking [22]. Moreover, TiO_2 can enhance opacity and brightness and it can improve the durability of the paint [23, 33].TiO_2 is a widely known pigment because of its

identical properties (including inert, stable, less costly and non-toxic) [24]. As an exceptional UV light absorber, TiO_2defenses from damage that occurs due to UV radiation [23,25]. Because of the identical features of TiO_2, medicinal products with very minute concentrations of pigment can reveal appealing shades and distinctive characteristics [24]. For tinting a variety of products in the cosmetics and pharmaceutical industries, TiO_2 is extensively used as a pigment [24,26, 35]. Across this industry, TiO_2 is employed to produce several products including lotions, shampoos, sunscreens, toothpaste and so on [27]. The prepared sample might be used for the pigments as well as for acrylic paint.

Conclusion

High crystallinephase 54.40% TiO_2 best-fitted strain anatase was synthesized at a very low temperature 60.0 $^{\circ}$C. Exhaustive parameters were investigated by X-ray diffraction (XRD) techniques employed for lattice parameters, crystal size, lattice volume, strain and weight fraction. 54.40 % anatase, 29.10 % brookite and 16.50 % rutile were found by WPPFmethod and lattice volume of anatase 137.150, brookite 267.079 and rutile 62.901 Å^3 as well the crystal strain 0.307, 0.45 and 0.28 % of anatase, brookite and rutile polymorph observedrespectively. The strain of the individual polymorphs of TiO_2 show best-fitted used for the pigment and acrylic paintfor its preferred orientation. The average crystallite size was 7.39 nm which confirmed the formation of nanocrystal-$TiO_2$and uniformly distribution into the medium. For the outstanding significant properties of the TiO_2polymorphsit could be very useful materials for the paint, wallpaper, colour-bank and pigment etc. industry.

Acknowledgement

The author's heartiest thanks to IPCRD, IGCRT, Division in Charge for using the software and computers.

Conflict of Interest

No known financial or personal interest could be influenced by this manuscript.

Data Availability

Data is available on request

Reference

[1] M. Laver, Chapter 10: titanium white, in: E.W. Fitzhugh (Ed.), Artists' Pigments: Volume 3: A Handbook of their History and Characteristics (pp. 295-355), National Gallery of Art, 1997http://dx.doi.org/10.2307/1506685.

[2] Du, P., Bueno-Lopez, A., Verbaas, M., Almeida, A. R., Makkee, M., Moulijn, J. A., & Mul, G. (2008). The effect of surface OH-population on the photocatalytic activity of rare earth-doped P25-TiO2 in methylene blue degradation. Journal of Catalysis, 260(1), 75-80.

[3] de Keijzer, M., de Groot, S., Megens, L., & Van Keulen, H. (2008). Schildertechnisch onderzoek aan Mondriaans Compositie met rood, zwart, geel en grijs uit 1920. Unpublished results. Instituut Collectie Nederland

[4] M. de Keijzer, The colourful twentieth century, in S. Fairbrass, J. Hermans (Eds.), Modern Art: The Restoration and Techniques of Modern Paper and Paints, United Kingdom Institute of Conservation, ISBN: 1871656044 1989, pp. 13–20.

[5] Van Driel, B. A., Kooyman, P. J., Van den Berg, K. J., Schmidt-Ott, A., & Dik, J. (2016). A quick assessment of the photocatalytic activity of TiO2 pigments—From lab to conservation studio! Microchemical Journal, 126, 162-171.

[6] M. de Keijzer, The history of modern synthetic inorganic and organic artists' pigments, in: J.A. Mosk, N.H. Tennent (Eds.), Contributions to Conservation: Research in Conservation at the Netherlands Institute for Cultural Heritage, James & James (Science Publishers) Ltd, ISBN: 1-902916-09-3, 2002.

[7] T.B. van Oosten, I. Fundeanu, C. Bollard, CastroC. d, A. Lagana, Lights out! The conservation of polypropylene wall tapestries, in B. Keneghan, L. Egan (Eds.), Plastics. Looking to the Future and Learning from the Past, Archetype Books, ISBN: 1904982433, 2008.

[8] T.F. Parsons, G.G. Gray, I.H. Crawford, To RC or not to RC, J. Appl. Photogr. Eng. 5 (2) (1979) 110–117.

[9] G. Völz Hans, G. Kaempf, G. Fitzky Hans, A. Klaeren, The chemical nature of chalking in the presence of titanium dioxide pigments, in: F.H. Winslow (Ed.), Photodegradation and Photostabilization of Coatings, ACS Symposium Series, American Chemical Society, 151 1981, pp. 163–182.

[10] T.A. Egerton, C.J. King, The influence of light intensity on photoactivity in TiO_2 pigmented systems, J. Oil Col. Chem. Assoc. 62 (1979) 386–391.

[11] Allen, N. S., Edge, M., Ortega, A., Sandoval, G., Liauw, C. M., Verran, J., ... & McIntyre, R. B. (2004). Degradation and stabilisation of polymers and coatings: nano versus pigmentary titania particles. Polymer degradation and stability, 85(3), 927-946.

[12] Khataee, A., & Mansoori, G. A. (2011). Nanostructured titanium dioxide materials: properties, preparation and applications. World Scientific.

[13] Jana, N. R., Gearheart, L., & Murphy, C. J. (2001). Seed- mediated growth approach for shape- controlled synthesis of spheroidal and rod- like gold nanoparticles using a surfactant template. Advanced Materials, 13(18), 1389-1393.

[14] Folli, A., Pade, C., Hansen, T. B., De Marco, T., & Macphee, D. E. (2012). TiO2 photocatalysis in cementitious systems: Insights into self-cleaning and de-pollution chemistry. Cement and concrete research, 42(3), 539-548.

[15] Gunschera, J., Markewitz, D., Bansen, B., Salthammer, T., & Ding, H. (2016). Portable photocatalytic air cleaners: efficiencies and by-product generation. Environmental Science and Pollution Research, 23, 7482-7493.

[16] Subbiah, G., Premanathan, M., Kim, S. J., Krishnamoorthy, K., & Jeyasubramanian, K. (2014). Preparation of TiO2 nano paint using ball milling process and investigation on its antibacterial properties. Materials Express, 4(5), 393-399.

[17] Alam, M. A., Bishwas, R. K., Mostofa, S., & Jahan, S. A. (2024). Low-temperature synthesis and crystal growth behavior of nanocrystal anatase-TiO2. Materials Letters, 354, 135396.

[18] Braun J H, Baidins A and Marganski R E 1992 TiO2 pigment technology: a review Progress in Organic Coatings 20 105–38

[19] Luttrell T, Halpegamage S, Tao J, Kramer A, Sutter E and Batzill M 2014 Why is anatase a better photocatalyst than rutile? - Model studies on epitaxial TiO2 films Sci Rep 4 4043

[20] Liu K, Cao M, Fujishima A and Jiang L 2014 Bio-Inspired Titanium Dioxide Materials with Special Wettability and Their Applications Chemical reviews 114

[21] Lied E, Morejon C, Basso R, Trevisan A, Bittencourt P and Fronza F 2018 Photocatalytic degradation of H 2 S in the gas-phase using a continuous flow reactor coated with TiO 2 -based acrylic paint Environmental Technology 40 1–24

[22] Fujishima A, Zhang X and Tryk D 2008 TiO2 Photocatalysis and Related Surface Phenomena Surface Science Reports 63 515–82

[23] Basso A, Battisti A P, Moreira R de F P M and José H J 2020 Photocatalytic effect of addition of TiO2 to acrylic-based paint for passive toluene degradation* Environmental Technology 41 1568–79

[24] Diebold M 2019 Optimizing the benefits of TiO2 in paints Journal of Coatings Technology and Research 17

[25] Wu X 2021 Applications of Titanium Dioxide Materials Titanium Dioxide - Advances and Applications (IntechOpen)

[26] Anon Titanium Dioxide - an overview | ScienceDirect Topics

[27] Lakshmanan V, Bhowmick A and Halim A 2014 Titanium Dioxide - Production, Properties and Applications p 75

[28] Anon Titanium Dioxide: Chemical Properties, Applications and Environmental Effects – Nova Science Publishers

[29] Alam, M. A., Munni, S. A., Mostafa, S., Bishwas, R. K., & Jahan, S. A. (2023). An Investigation on Synthesis of Silver Nanoparticles. Asian Journal of Research in Biochemistry, 12(3), 1-10.

[30] Alam, M. A., Mobashsara, M. T., Sabrina, S. M., Bishwas, R. K. B., Debasish, D. S., & Shirin, S. A. J. (2023). One-pot Low-Temperature Synthesis of High Crystalline Cu Nanoparticles. Malaysian Journal of Science and Advanced Technology, 122-127.

[31]Alam, M. A., Tabassum, M., Mostofa, S., Bishwas, R. K., Sarkar, D., & Jahan, S. A. (2023). The effect of precursor concentration on the crystallinity synchronization of synthesized copper nanoparticles. Journal of Crystal Growth, 621, 127386.

[32]Tabassum, M., Alam, M. A., Mostofa, S., Bishwas, R. K., Sarkar, D., & Jahan, S. A. (2024). Synthesis and crystallinity integration of copper nanoparticles by reaction medium. Journal of Crystal Growth, 626, 127486.

[33] Gupta, T., Cho, J., & Prakash, J. (2021). Hydrothermal synthesis of TiO2 nanorods: formation chemistry, growth mechanism, and tailoring of surface properties for photocatalytic activities. Materials Today Chemistry, 20, 100428.

[34]Sharma, A., Karn, R. K., & Pandiyan, S. K. (2014). Synthesis of TiO2 nanoparticles by sol-gel method and their characterization. J Basic Appl Eng Res, 1(9), 1-5.

[35]Zhang, Y., Liu, Z., Zhang, X., Wang, Q., Wang, Q., Wang, H., ... & Liu, J. (2021). The formation mechanism of (001) preferred orientation for anatase TiO2 film prepared by DC pulsed magnetron sputtering. Vacuum, 190, 110287.

[36] Moulick, S. P., Hossain, M. S., Al Mamun, M. Z. U., Jahan, F., Ahmed, M. F., Sathee, R. A., ... & Islam, F. (2023). Characterization of waste fish bones (Heteropneustes fossilis and Otolithoides pama) for photocatalytic degradation of Congo red dye. Results in Engineering, 20, 101418.

[37]Bishwas, R. K., Mostofa, S., Alam, M. A., & Jahan, S. A. (2023). Removal of malachite green dye by sodium dodecyl sulfate modified bentonite clay: Kinetics, thermodynamics and isotherm modeling. Next Nanotechnology, 3, 100021.

[38]Saqib, M., Rahman, N., Safeen, K., Mekkey, S. D., Salem, M. A., Safeen, A., ... & Khan, R. (2023). Structure phase-induced photodegradation properties of cobalt-sulfur co-doped TiO2 nanoparticles synthesized by hydrothermal route. Journal of Materials Research and Technology, 26, 8048-8060.

[39] Rahman, M. M., Maniruzzaman, M., Yeasmin, M. S., Gafur, M. A., Shaikh, M. A. A., Alam, M. A., ... & Quddus, M. S. (2023). Adsorptive abatement of Pb2+ and crystal violet using chitosan-modified coal nanocomposites: A down flow column study. Groundwater for Sustainable Development, 23, 101028.

[40]Ramadan, M., Kohail, M., Abadel, A. A., Alharbi, Y. R., Soliman, A. M., & Mohsen, A. (2023). Exploration of mechanical performance, porous structure, and self-cleaning behavior for hydrothermally cured sustainable cementitious composites containing de-aluminated metakaolin waste and TiO2 nanoparticles. Journal of Materials Research and Technology.

[41] Govind, B., Bharti, P., Srivastava, M., Kumar, A., Bano, S., Bhatt, K., ... & Misra, D. K. (2021). Magnetic properties of intermediate Ni2-xMn1+ xSb full-Heusler compounds. Materials Research Bulletin, 142, 111427.

[42]Govind, B., Srivastava, M., Pulikkotil, J. J., & Misra, D. K. (2021). Electronic structure and magnetic properties of a full-Heusler Mn2NiSb: Cu2MnAl type structure. Journal of Magnetism and Magnetic Materials, 517, 167375.

[43]Qin, D. D., Bi, Y. P., Feng, X. J., Wang, W., Barber, G. D., Wang, T., ... & Mallouk, T. E. (2015). Hydrothermal growth and photoelectrochemistry of highly oriented, crystalline anatase TiO2 nanorods on transparent conducting electrodes. Chemistry of Materials, 27(12), 4180-4183.